Journal of Macromolecular Science, Part A
Publication details, including instructions for authors and subscription information:
http://www.informaworld.com/smpp/title~content=t713597274

THERMALLY STABLE NLO MATERIALS BASED ON ORGANOSOLUBLE POLYIMIDES AND AN ALKOXYSILANE DYE VIA SOL-GEL PROCESS

Ru-Jong Jeng[a]; Li-Hsin Jan[a]; Rong-Ho Lee[b]
[a] Department of Chemical Engineering, National Chung Hsing University, Taichung, Taiwan, ROC [b] Industrial Technology Research Institute, Hsinchu, Taiwan, ROC

To cite this Article Jeng, Ru-Jong , Jan, Li-Hsin and Lee, Rong-Ho(2001) 'THERMALLY STABLE NLO MATERIALS BASED ON ORGANOSOLUBLE POLYIMIDES AND AN ALKOXYSILANE DYE VIA SOL-GEL PROCESS', Journal of Macromolecular Science, Part A, 38: 8, 821 — 837

To link to this Article: DOI: 10.1081/MA-100104450

URL: http://dx.doi.org/10.1081/MA-100104450

J. MACROMOL. SCI.—PURE APPL. CHEM., A38(8), 821–837 (2001)

THERMALLY STABLE NLO MATERIALS BASED ON ORGANOSOLUBLE POLYIMIDES AND AN ALKOXYSILANE DYE VIA SOL-GEL PROCESS

Ru-Jong Jeng,[1],* Li-Hsin Jan,[1] and Rong-Ho Lee[2]

[1]Department of Chemical Engineering, National Chung Hsing
University, Taichung 402, Taiwan, ROC
[2]Opto-Electronics & Systems Lab., Industrial Technology Research
Institute, Chutung, Hsinchu 310, Taiwan, ROC

ABSTRACT

A series of organic-inorganic materials based on organosoluble polyimides and an alkoxysilane dye for second-order nonlinear optics have been developed. A sol-gel reaction of a nonlinear optically active alkoxysilane dye (ASD) is utilized to grow a network in polymer matrices or create an interpolymer network among polyimide chains. SEM results indicate that the inorganic networks are distributed uniformly throughout the polymer matrices on the molecular scale. The silica particle sizes are well under 1 µm. Second harmonic coefficients, d_{33} of 8.4 to 47.6 pm/V have been obtained for the poled/cured polyimide/ASD samples. Excellent temporal stability was obtained for these NLO materials at 100°C. The composition effect on the second order nonlinearity is also reported.

Key Words: Nonlinear optics; Polyimide; Sol-gel process; Organic-inorganic.

INTRODUCTION

Polymeric materials with large and stable second-order nonlinear optical (NLO) coefficient are of interest for their potential use in electrooptic applications

---

*Corresponding author.

[1-2]. To prevent the randomization of the poled molecules, NLO chromophore are usually incorporated into either high glass transition temperature (T_g) polymers and/or crosslinked polymer networks [3-9].

Aromatic polyimides are well-known for their high temperature stability and high glass transition temperatures [10]. Several approaches have been reported to enhance the stability and processability of NLO materials based on polyimides [11-14]. Jeng and coworkers have reported a second-order NLO organic/inorganic composite based on an alkoxysilane dye and an aromatic polyimide [12]. Polyimide films containing a homogeneous dispersion of SiO_2 particles have been achieved by means of a sol-gel process. This sol-gel process involves the sequential hydrolysis and polycondensation of alkoxysilane at temperatures that are commonly used to process polymeric materials [15-16]. The internal production of water due to the curing of polyamic acid aids the hydrolysis of the alkoxysilane. Moreover, the carboxylic acid group of the polyamic acid, being a Brönsted acid, might have a catalytic effect on hydrolysis and polycondensation of alkoxysilane. The incorporation of an inorganic sol-gel material provides an inert environment for the polyimide and, theoretically will prevent its thermal decomposition. The inorganic networks will be densely and uniformly packed throughout the organic chain segments by the sol-gel process [17]. Apart from high T_g of polyimides, the interactions between inorganic oxide particles and polyimide will reduce the molecular motions during the glass transition [17]. Therefore, the incorporation of an inorganic NLO sol-gel material within an organic polymer can effectively enhance long-term NLO stability at elevated temperatures.

On the basis of the above considerations, polyimides possessing both high T_g and a crosslinked network seem to be a reasonable approach to enhance the stability. Organosoluble polyimides may be used to circumvent the need for thermal imidization. Improved processability is achieved without sacrificing useful properties, such as excellent thermal stability and mechanical property [18]. As part of an endeavor in pursuing long-term NLO stability, we have reported preliminary results on a system of the organosoluble polyimides and an alkoxysilane dye [14]. Further study on the relationship between the chemical structure and NLO stability, and the composition effect on the temporal stability and relaxation behavior of the NLO property is one of the critical issues to pursue device-quality materials.

In this investigation, we report a series of the organic-inorganic NLO materials based on an alkoxysilane dye (ASD) and two organosoluble polyimides (PIA and PIB) via the sol-gel process. During sol-gel reaction, NLO-active inorganic networks were grown *in situ* in polyimide matrices. It is important to note that covalent bonding is available only for PIB-ASD sample via formation of phenoxysilicon linkages [9]. Thermal behaviors of these organic-inorganic NLO materials were studied with DSC and TGA, respectively. Phase homogeneity was analyzed using scanning electron microscopy (SEM). Furthermore, the composition effect on the temporal stability and relaxation behavior of the NLO property was studied in detail.

EXPERIMENTAL

Aromatic organosoluble polyimide A (PIA) and polyimide B (PIB) (Figure 1) were successfully by solution imidization techniques [19]. There is no hydroxyl group on PIA, whereas PIB has lateral hydroxyl groups on the backbones. α,α'-Bis-(4-aminophenol)-1,4-diisopropylbenzene (Bis-P), 4,4'-oxydiphthalic anhydride (ODPA), and 2,2-Bis(3-amino-4-hydroxyphenyl)-hexafluoropropane (BAPAF) are available from TCI Co. and used as received. The alkoxysilane dye (ASD; Scheme 1) was synthesized by the coupling of a monoepoxy of (3-glycidoxypropyl) trimethoxysilane and a monoamine of 4-[(4'-nitrophenyl)azo]aniline (Disperse Orange 3) [20]. The crosslinking of these sol-gel materials was characterized by the Fourier transform infrared (FTIR) spectroscopy (Bio-Rad FTS155 FTIR). T_g's were determined using differential scanning calorimetry (DSC; Seiko SSC/5200) at a heating rate of 10°C/min. Degradation temperatures (T_d) were measured on a Seiko Exstar 6000 thermogravimetric analyzer (TGA) at 10°C/min. under air. UV-vis spectra were recorded on a Perkin Elmer Lambda 2S spectrophotometer. SEM (Jeol JEM-840A) was used to study the morphology of the polymer film (gold coated).

A polymer solution containing ASD and polyimide was prepared for spin-coating. PIA and PIB were respectively dissolved in the chloroform and THF with ASD in different weight ratios (10/90, 30/70, 50/50, 70/30, 90/10 wt%) containing 10 mg of 90% methanoic acid to aid the hydrolysis of ASD. The polymer solution was stirred at room temperature for 3 hours. Thin films were prepared by spin-coating the polymer solution onto indium tin oxide (ITO) glass substrates. The poling process for the second-order NLO polymer films was carried out using an *in situ* poling technique. The details of the corona poling set-up were the same as was reported earlier [21]. The poling process was started at room temperature and increased to 160°C at heating rate of 15°C/min. The corona current was maintained at 4 μA with a potential of 5.5 kV while the poling temperature was kept at 160°C for 2 hours. The formation of the network and the molecular alignment of

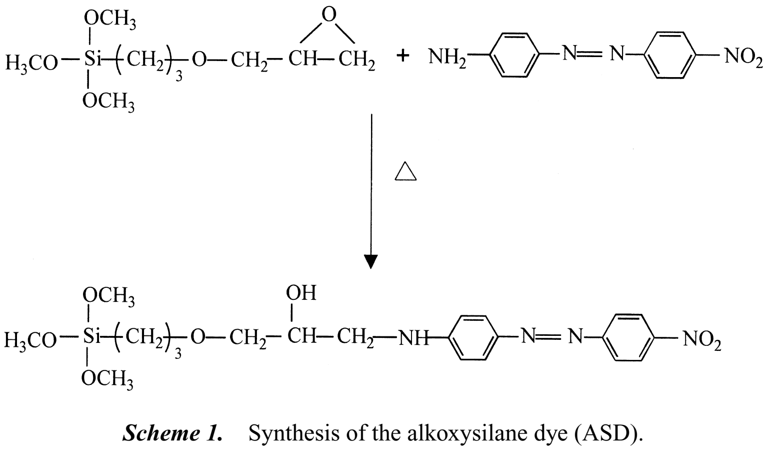

Scheme 1. Synthesis of the alkoxysilane dye (ASD).

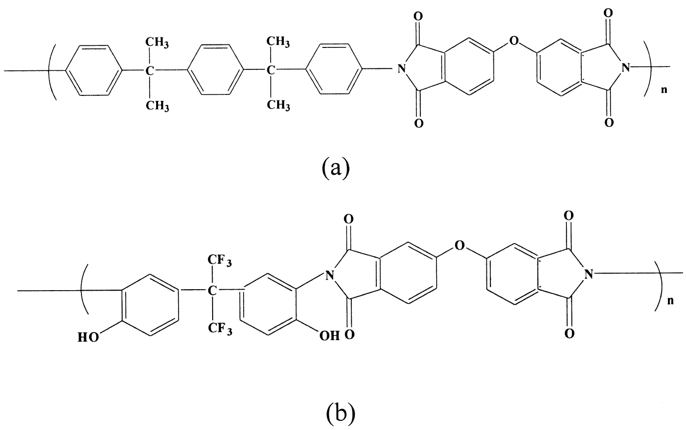

Figure 1. Chemical structures of (a) PIA and (b) PIB.

the poled order proceeded simultaneously during this period. Upon saturation of the SHG signal intensity, the sample was then cooled down to room temperature in the presence of the poling field at which point the poling field was terminated. The thickness and indices of refraction were measured by a prism coupler (Metricon 2010) for the NLO polymer films. Second harmonic generation measurements were carried out with a Q-switched Nd:YAG laser operating at 1064 nm. Measurement of the second harmonic coefficient, d_{33}, has been previously discussed [22], and the d_{33} values were corrected for absorption [23].

RESULTS AND DISCUSSION

The curing conditions were determined using a DSC reaction scan for the sol-gel process. Moreover, to optimize the poling temperature and investigate the chromophore stability in the polyimide, an UV-vis spectrophotometer was utilized to trace the chromophore. Figure 2 shows absorption characteristic of the PIA50 sample thermal-treated at various temperatures for 1 hour. A sharp decrease of the absorbance was observed when temperatures were higher than 180°C. It is important to note that no detectable decay of UV intensity was observed after thermal treatment at 170°C for 24 hours. Therefore, an optimum curing/poling condition of polyimide/ASD samples was chosen to be at 160°C for 2 hours due to the consideration of the thermal stability of ASD and effective alignment of the NLO chromophores. Figure 3 shows the FTIR spectra of the PIB, ASD, and cured PIB50 (PIB:ASD = 50:50) samples. For the cured PIB50 sample, the broadening absorption peak at around 1100 cm^{-1} was identified as the formation of Si-O-Si network resulted from sol-gel reaction among ASD molecules [12]. This was also observed in the FTIR spectra of the cured PIA/ASD samples. The appearance of phenoxysilicon bond absorption at 960 cm^{-1} for the cured PIB50 indicates the formation of covalent bonds between polyimide and ASD has occurred. Moreover,

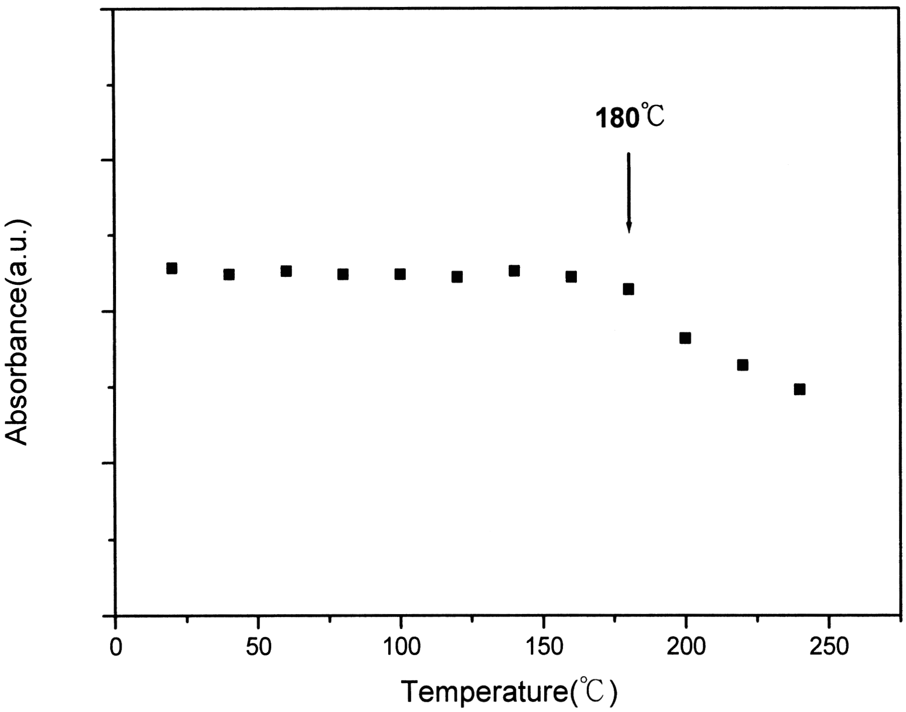

Figure 2. Thermal stability of the PIA50 measured by an UV-vis spectrophotometer.

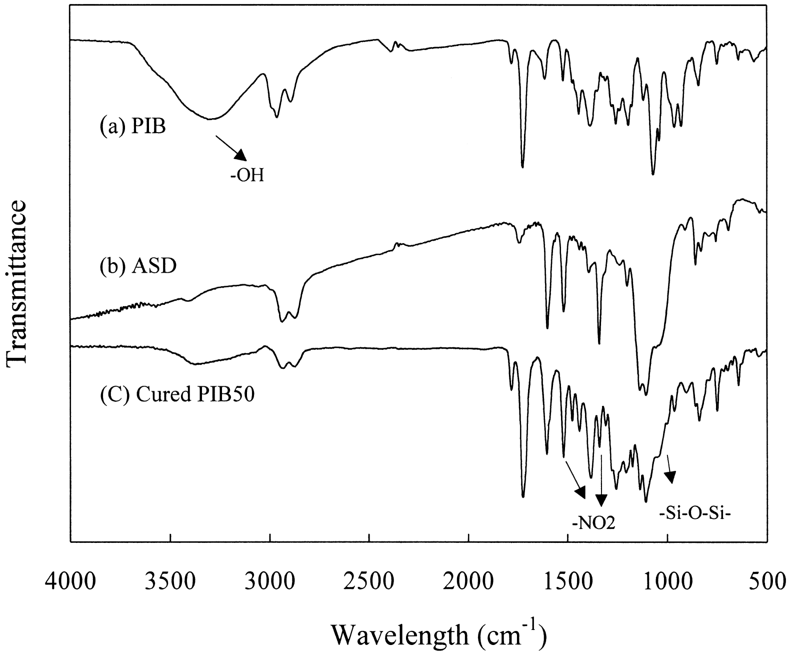

Figure 3. Infrared spectra of the (a) PIB; (b) ASD; and (c) cured PIB50.

the absorption peak of hydroxyl stretching around 3400 cm^{-1} decreased drastically after curing. This further supports the formation of the phenoxysilicon linkages. However, the phenoxysilicon bond absorption was not observed for the cured PIA/ASD samples due to the fact that there is no hydroxyl group on PIA. To further understand the degree of crosslinking reaction among ASD molecules in polyimide, the silica network of PIA50 was characterized by ^{29}Si NMR (Figure 4). Two major absorption peaks were observed and assigned to monohydroxy-substituted silica (T_2) and nonhydroxy-substituted silica (T_3). The stronger absorption intensity of T_3 indicates that most of the silicons are bound to two other silicons through the oxygen bridges for the PIA50 sample [24].

T_g's of the polyimide/inorganic materials were measured on the DSC after curing at 160°C for 2 hours. T_g's of PIA and PIB were observed at temperature of 230°C and 232°C, respectively. The hydrogen bonding of lateral hydroxyl group on the backbone of PIB doesn't results in a higher T_g as compared to PIA. For the cured PIA/ASD and PIB/ASD samples, T_g's of such organic-inorganic materials were enhanced significantly as the incorporation of the ASD into the polymer matrices. A broad glass transition was observed at temperatures around 290°C for both the cured PIA70 (PIA: ASD = 70:30 wt%) and PIB90 (PIB: ASD = 90:10 wt%) samples as shown in Figure 5. Less ASD content of PIB90 has the same temperature range of T_g of PIA70. This is due to the fact that the methoxyl groups of ASD reacted with the aromatic hydroxyl groups of PIB to form crosslinked NLO-active polyimide [9], whereas the sol-gel reaction of ASD within PIA matrices form an organic/inorganic composite. However, T_g's were not detectable from the DSC study for the cured PIA/ASD and PIB/ASD samples with a higher ASD content because of the formation of high crosslinking density of the organic and inorganic networks [25]. In addition, thermal decomposition behavior was measured on a TGA under air after curing at 160°C for 2 hours. T_d was read at the

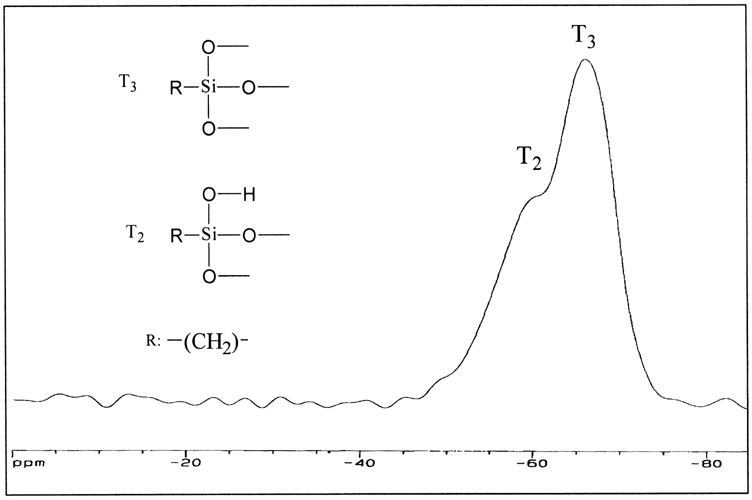

Figure 4. ^{29}Si spectrum of the cured PIA50 sample.

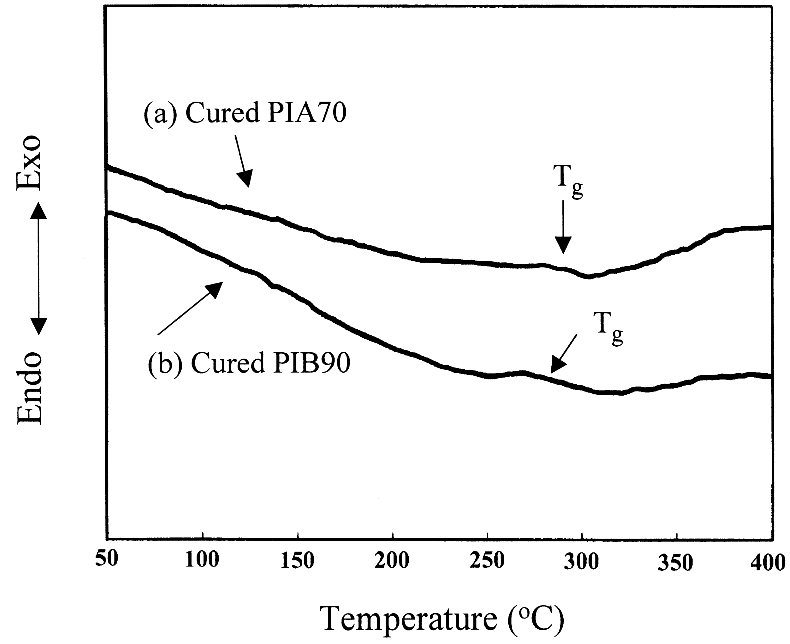

Figure 5. DSC thermograms of the cured PIA70 and PIB90.

temperature corresponding to the weight loss of 5%. The compositions and T_d's of the polyimides and polyimide/inorganic materials are summarized in Table 1. T_d's were observed at temperature above 370°C for both the PIA and PIB. Moreover, T_d's of the PIA/ASD and PIB/ASD samples were observed in the range of 255 to 285°C. The composition effect on the T_d was not significant for these NLO mate-

Table 1. Thermal Degradation Temperatures of the Polyimides and ASD Based NLO Materials

Samples[a]	Composition (weight ratio)	T_d^b (°C)
PIA	PIA/ASD(100/0)	463.3
PIA90	PIA/ASD(90/10)	255.1
PIA70	PIA/ASD(70/30)	270.0
PIA50	PIA/ASD(50/50)	272.1
PIA30	PIA/ASD(30/70)	265.7
PIA10	PIA/ASD(10/90)	263.5
PIB	PIB/ASD(100/0)	374.5
PIB90	PIB/ASD(90/10)	275.3
PIB70	PIB/ASD(70/30)	276.3
PIB50	PIB/ASD(50/50)	284.8
PIB30	PIB/ASD(30/70)	275.9
PIB10	PIB/ASD(10/90)	267.8
ASD	PIB/ASD(0/100)	247.2

[a] Samples were cured at 160°C for 2 hours.
[b] T_d was read at the temperature corresponding to 5% wt loss.

rials. However, the cured polyimide/ASD samples have a higher T_d than that of the cured ASD ($T_d = 247$). It is important to note that the 5%wt loss of the NLO materials mostly results from either further sol-gel reaction (i.e., condensation) of residual silanol groups [26], or degradation of the NLO moieties (i.e., azobenzene). The homogeneity of these organic-inorganic materials was studied using SEM. The fractured surfaces of the cured PIA90, PIA50, and PIA10 are shown in Figure 6. No sign of any phase separation was observed when magnification was increased up to 5 K. In addition, the distribution of inorganic networks in the polymer matrix has been further confirmed using SEM with a mapping technique

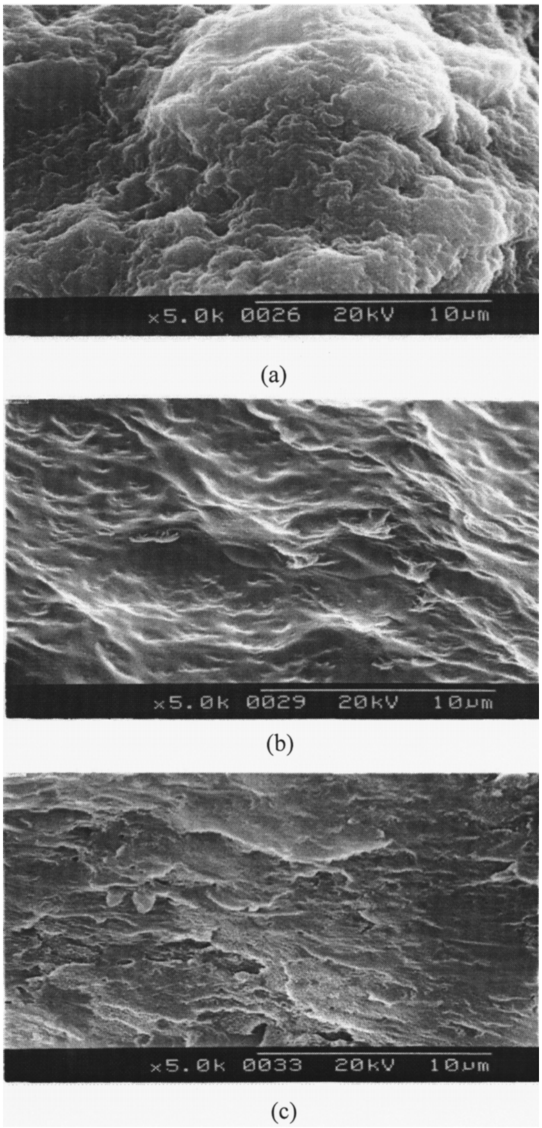

(a)

(b)

(c)

Figure 6. Scanning electron micrographs of the cured (a) PIA90, (b) PIA50, and (c) PIA10.

[27]. The mapping spectra of the cured PIA90, PIA50, and PIA10 are shown in Figure 7. The results indicate that the silicons are distributed uniformly throughout the polymer film. It is important to note that the silica particle sizes are much smaller than 1 mm for these samples due to complete transparency of the sample [28]. The observation by SEM supports that a high degree of uniform mixing

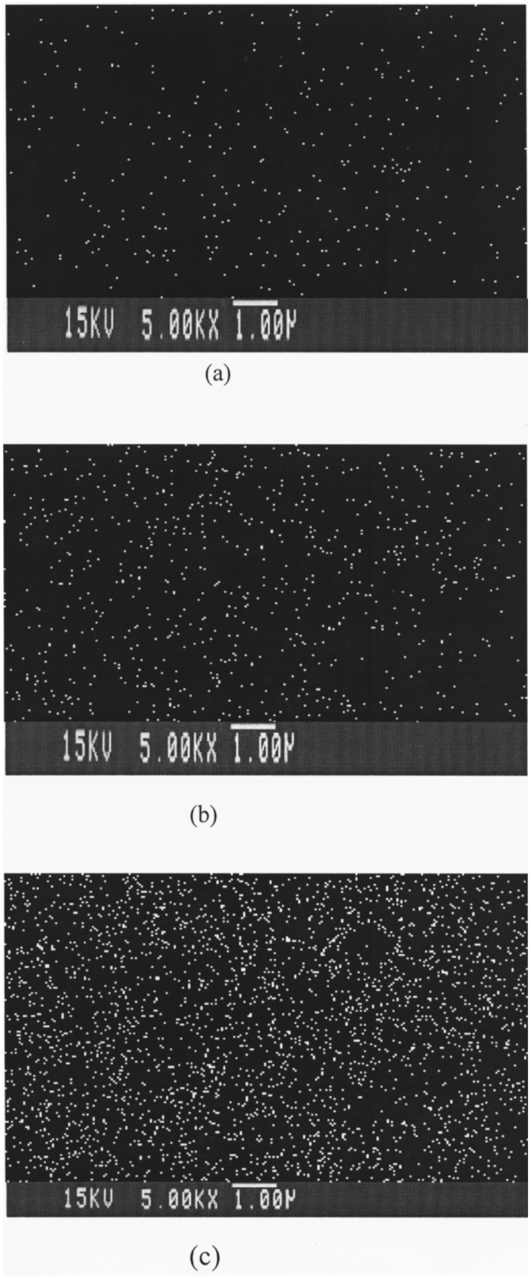

Figure 7. SEM mapping micrographs of the cured (a) PIA90, (b) PIA50, and (c) PIA10, respectively.

between the polymer chains and inorganic networks was obtained for these polyimide and ASD based materials.

To investigate the absorption behavior as a function of time, the absorption spectra (Figure 8) was taken regularly over 170 hours period under thermal treatment at 100°C for the poled/cured PIA50 and PIB50 samples. The maximum of the absorption was located around 460 nm and 475 nm for the PIA50 and PIB50, respectively. Immediately after poling/curing, a decrease in absorption and a blue shift were observed in the spectrum. This was due to dichroism and elec-

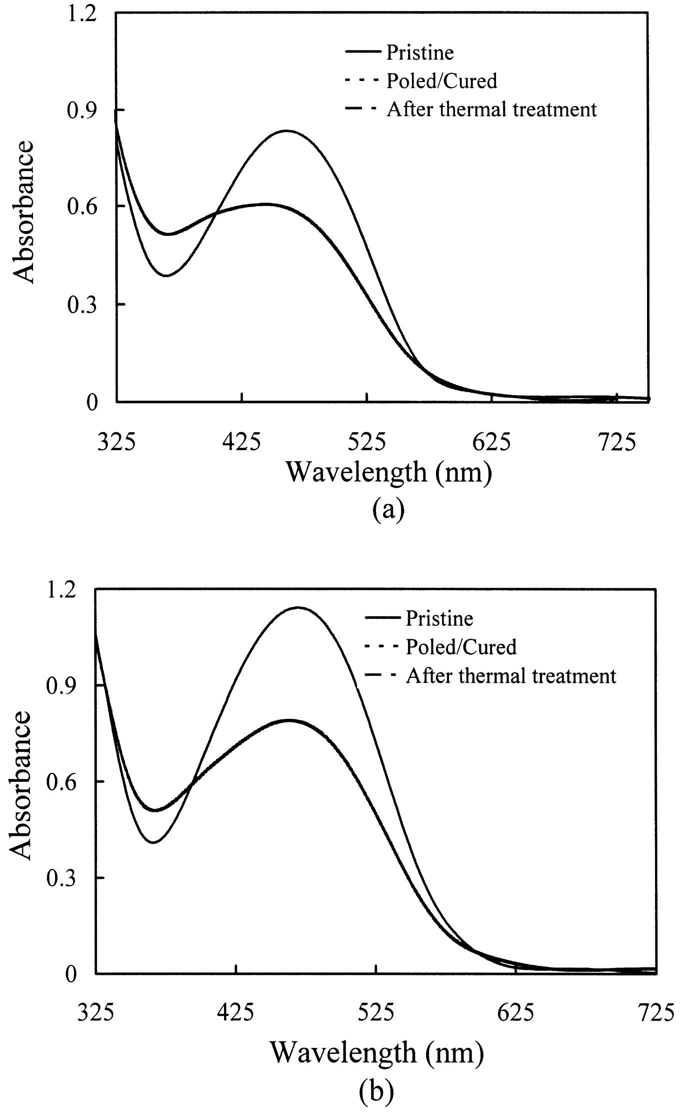

Figure 8. UV/vis absorption spectra of the (a) PIA50, and (b) PIB50.

Table 2. Thickness and Refraction Indices of the Polyimides and ASD Based NLO Materials

Samples[a]	d(μm)[b]	n_{543}[c]	n_{633}	n_{830}
ASD	1.1	1.72	1.68	1.65
PIA10	1.2	1.71	1.69	1.64
PIA30	1.1	1.71	1.68	1.65
PIA50	0.9	1.66	1.64	1.63
PIA70	1.4	1.66	1.63	1.60
PIA90	1.2	1.66	1.65	1.63
PIB10	1.5	1.68	1.66	1.64
PIB30	1.2	1.77	1.75	1.73
PIB50	1.7	1.67	1.64	1.62
PIB70	1.1	1.64	1.63	1.59
PIB90	1.2	1.69	1.67	1.65

[a] Samples were cured at 160°C for 2 hours.
[b] d: the thickness of polymer film.
[c] n_{543}, n_{633}, n_{830}: refraction indices at 543, 633, and 830 nm, respectively.

trochromism resulting from the induced dipole alignment [29]. During the next 170 hours, the absorption spectra remained unchanged for both samples. The linear optical properties of these NLO sol-gel materials are summarized in Table 2. The thickness of the polymer films ranged from 0.9 to 1.7 μm. The refraction indices ranged from 1.59 to 1.72, and increase with an increasing content of ASD. The second-harmonic coefficients d_{33} and d_{31} of poled/cured ASD, PIA/ASD, and PIB/ASD samples for incident light of 1064 nm are summarized in Table 3. These polyimide/ASD based materials show large second-order nonlinearity after poling and curing at 160°C for 2 hours. Moreover, the second-harmonic coefficients increase with increasing content of ASD.

The temporal characteristics of the effective second harmonic coefficients (d_{eff}) for the poled/cured ASD, PIA/ASD, and PIB/ASD samples at 100°C are shown in Figure 9. A much better temporal stability was obtained for the

Table 3. Second Harmonic Coefficients d_{33} and d_{31} (pm/V) of the Poled/Cured Polyimides and ASD Based NLO Materials at 1064 nm

Samples	$d_{33(1064)}$	$d_{31(1064)}$
ASD	54.0	19.2
PIA10	47.6	14.2
PIA30	34.5	9.7
PIA50	28.9	8.2
PIA70	15.8	4.7
PIA90	9.7	3.8
PIB10	43.7	15.6
PIB30	33.6	11.3
PIB50	27.8	8.4
PIB70	11.6	4.7
PIB90	8.4	3.1

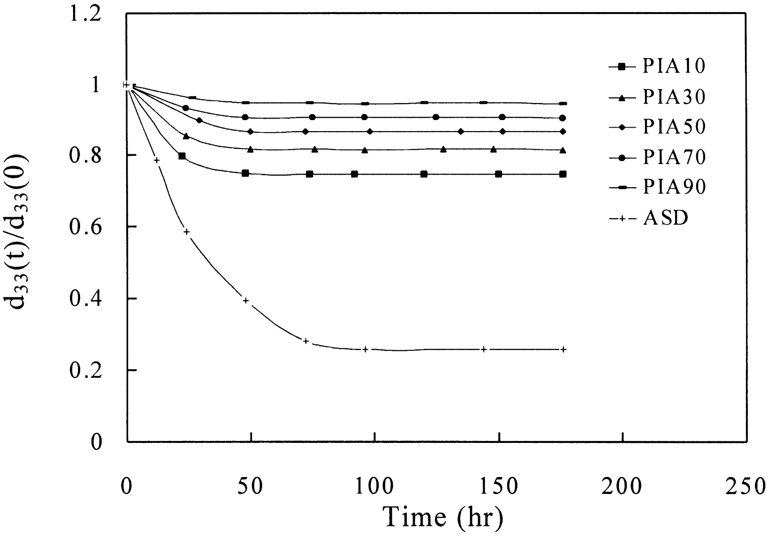

(a)

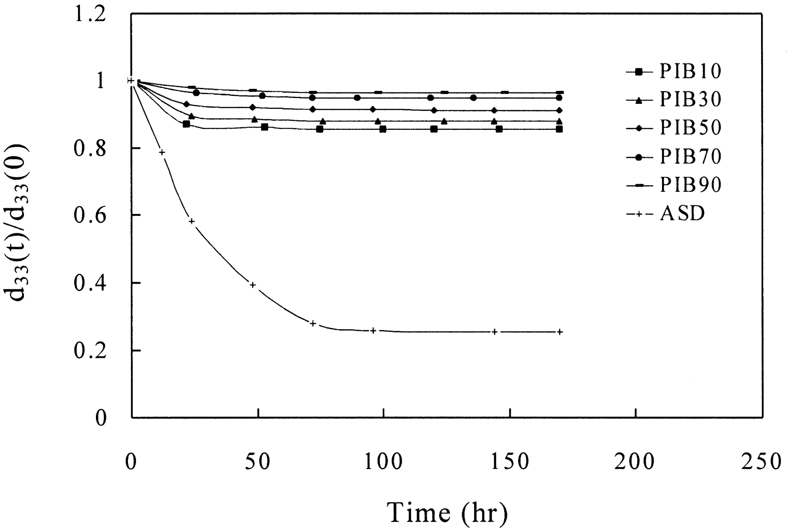

(b)

Figure 9. Temporal behavior of the second-order NLO coefficient for the poled/cured (a) PIA/ASD, and (b) PIB/ASD samples at 100°C.

poled/cured polyimide/ASD samples as compared to the poled/cured ASD. After being subjected to thermal treatment at 100°C for 168 hours, a reduction of less than 30% in the d_{eff} was observed for all of the poled/cured PIA/ASD samples. On the other hand, a reduction of less than 20% in the d_{eff} was observed for all of the poled/cured PIB/ASD samples. The temporal stability was increased with decreasing content of ASD. In comparison with the poled/cured PIA/ASD sam-

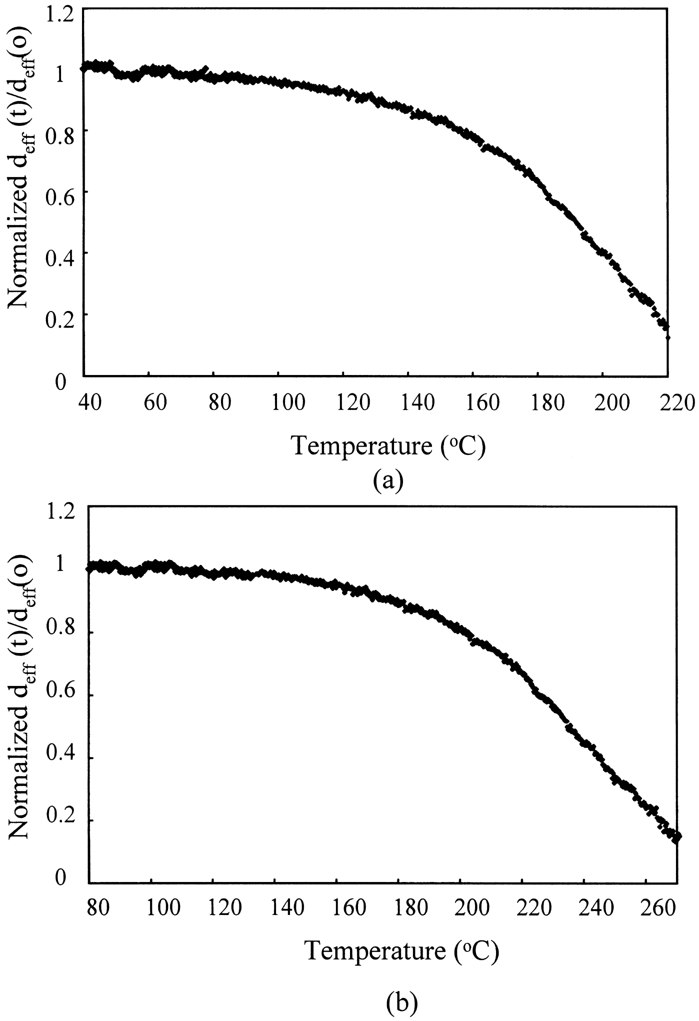

Figure 10. Temperature dependence of the dipole re-orientational dynamics of (a) the poled/cured PIA/ASD50 (o) and (b) PIB/ASD50 (x).

ples, the poled/cured PIB/ASD samples exhibited better temporal stability. This is direct consequence of inter-polymer chain crosslinking in the cured PIB/ASD samples. In general, the SH signal of NLO polymers remained stable at low temperatures, but decayed significantly at a specific temperature. This specific temperature is defined as the effective relaxation temperature, T_0.[30, 31] The T_0 value provides information on maximum device operating temperatures that the film can endure, and allows quick evaluation of the temporal and thermal stability of the materials. Figure 10 shows the dynamic NLO thermal stability of the poled/cured PIA50 and PIB50 samples. It is important to note that the T_0 (190°C) of PIB50 is much hihger than that (150°C) of PIA50. This is due to the presence of the above-mentioned inter-chain crosslinking between PIB and ASD inorganic network. The inter-chain crosslinking further restricts molecular motion, and subsequently leads to better temporal stability.

Decay of the second harmonic coefficient is further described by the Kohlrausch-Williams-Watts function (KWW) for the poled/cured polyimide/ASD samples [32]

$$d_{33}(t)/d_{33}(0) = \exp^{-(t/\tau)\beta}$$

where τ represents the relaxation time, and broadening parameter β is a constant between 0 and 1, which characterizes the parameter of the relaxation time distribution. The composition effect on the relaxation time of the poled/cured polyimide/ASD samples is shown in Figure 11. The relaxation time was increased with increasing content of polyimide. High temperature results in fast decay of second

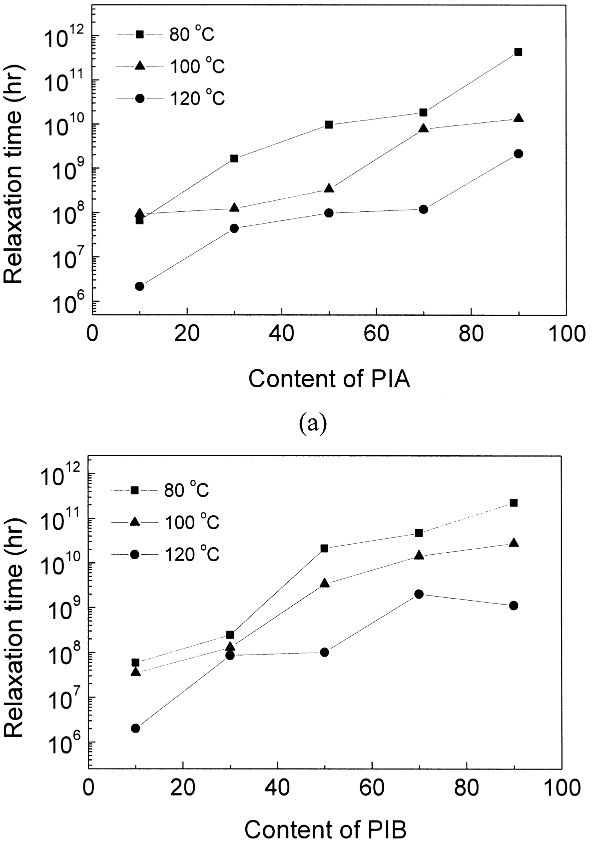

(a)

(b)

Figure 11. Relaxation time vs. polyimide content for the poled/cured (a) PIA/ASD, and (b) PIB/ASD samples at different temperatures.

harmonic coefficient, which has a short relaxation time for the poled/cured polyimid/ASD samples. The value of the broadening parameter was increased with increasing content of ASD (Figure 12). This is due to the fact that the NLO chromophore was more easily to be poled under the electric filed for the polyimide/ASD sample with a low T_g and high content of ASD. High poling efficiency results in a high degree and uniform alignment of the NLO chromophores, which has a narrow distribution of the relaxation time. As a result, high value of β was obtained for the sample with a high ASD content. In addition, an increase in the broadening parameter as a function of temperature reflects a gradual narrowing distribution of the relaxation time. As the temperature increases, the molecular mobility of the each NLO chromophore reaches the same level, which results in the gradual narrowing distribution of the relaxation time [33].

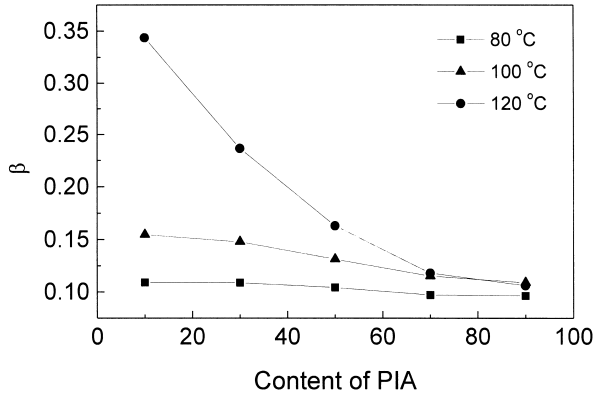

(a)

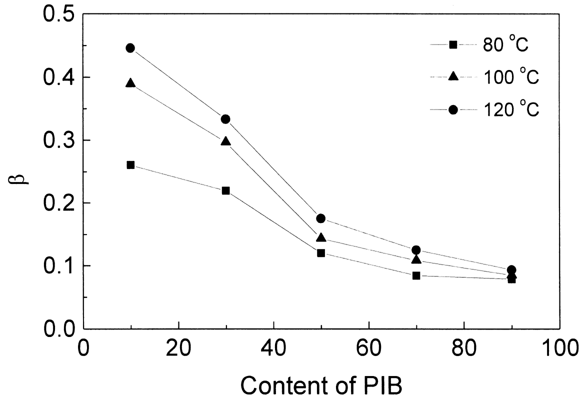

(b)

Figure 12. Broadening parameter vs. polyimide content for the poled/cured (a) PIA/ASD, and (b) PIB/ASD samples at different temperatures.

CONCLUSION

A series of the organosoluble polyimides (PIA and PIB) and ASD based organic-inorganic NLO materials via sol-gel process have been developed. Large second-order nonlineraity was obtained after poling and curing at 160°C for 2 hours. The methoxyl groups of ASD was reacted with the aromatic hydroxyl groups of PIB to form crosslinked NLO-active polyimide, whereas the sol-gel reaction of ASD within PIA matrices to form an organic/inorganic composite. This results in a better temporal stability of the poled/cured PIB/ASD samples as compared to that of the poled/cured PIA/ASD samples. The temporal stability was also affected by the composition of the polyimide/ASD samples, which was increased with decreasing content of ASD. In addition, the relaxation of the second harmonic coefficient was further described by the Kohlrausch-Williams-Watts function. The relaxation time and broadening parameter are temperature- and composition-dependent for these Polyimide-inorganic NLO materials. Future work involves the synthesis of double-end crosslinkable ASD and the incorporation of chromophore into organosoluble polyimide mainchains to further enhance the nonlinearity as well as temporal stability [34, 35].

ACKNOWLEDGMENT

The authors thank the National Science Council of Taiwan, ROC, for financial support (Grant NSC89-2216-E-005-002).

REFERENCES

1. Prasad, P.N.; Williams, D.J. *Introduction to Nonlinear Optical Effects in Molecules and Polymers,* John Wiley & Sons, Inc.: New York, 1991.
2. Singer, K.D.; Sohn, J.E.; Lalama, S. J. Appl. Phys. Lett. **1986**, *49*, 248.
3. Meredith, G.R.; Dusen, J.G.; Williams, D.J. Macromolecules **1982**, *15*, 1385.
4. Wang, N.P.; Leslie, T.M.; Wang, S.; Kowel, S.T. Chem. Mater. **1995**, *7*, 185.
5. Stenger-Smith, J.D.; Henry, R.A.; Hoover, J.M.; Lindsay, G.A.; Nadler, M.P. Nissan, R.A. J. Polym. Sci., Polym. Chem. **1993**, *31*, 2899.
6. Xu, C.; Wu, B.; Todorova, O.; Dalton, L.R.; Shi, Y.; Ranon, P.M.; Steier, W.H. Macromolecules **1993**, *26*, 5303.
7. Jeng, R.J.; Chen, Y.M.; Jain, A.; Tripathy, S.K.; Kuman, J. Optics Commun. 1992, *89*, 212.
8. Kim, J.; Plawsky, J.L.; LaPeruta, R.; Korenowski, G.M. Chem. Mater. **1992**, *4*, 249 .
9. Jeng, R.J.; Chen, Y.M.; Chen, J.I.; Kumar, J.; Tripathy, S.K. Macromolecules **1993**, *26*, 2530.
10. Marturunkakul, S.; Chen, J.I,; Jeng, R.J.; Sengupta, S.; Kumar, J.; Tripathy, S.K. Chem. Mater. **1993**, *5*, 743.
11. Wu, J.W.; Valley, J.F.; Ermer, S.; Binkley, E.S.; Kenney, J.T.; Lipscomb, G.F. Lytel, R. Appl. Phys. Lett. **1991**, *58*, 225.

12. Jeng, R.J.; Chen, Y.M.; Jain, A.K.; Kumar, J.; Tripathy, S.K. Chem. Mater. **1992**, 4, 1141.
13. Lin, J.T.; Hubbard, M.A.; Marks, T.J.; Lin, W.; Wong, G.K. Chem. Mater. **1992**, *4*, 1148.
14. Hsiue, G.H.; Kuo, J.K.; Jeng, R.J. Chem. Mater. **1994**, *6*, 884.
15. Updegraff, I.H. In '*Encyclopedia of Polymer Science and Engineering*', John Wiley & Sons, Inc.: New York, 1986.
16. Jeng, R.J.; Hsiue, G.H.; Chen, J.I.; Marturunkakul, S.; Li, L.; Jiang, X.L.; Moody, R.; Masse, C.; Kumar, J.; Tripathy, S.K. J. Appl. Polym. Sci. **1995**, *55*, 209.
17. Landry, C.J.T.; Coltrain, B.K.; Wesson, J.A.; Zumbulyadis, N.; Lippert, J.L. Polymer **1992**, *33*, 1496.
18. Glatz, F.P.; Mulhaupt, R. Polym. Bull. **1993**, *31*, 131.
19. Lakshmanan, P.; Srinivasan, S.; Moy, T.; McGrath, J. E. Polym. Prepr. Am. Chem. Soc., Div. Polym. Chem. **1993**, *34*, 707.
20. Mandal, B.; Jeng, R.J.; Kumar, J.; Tripathy, S.K. Makromol. Chem., Rapid Commun. **1991**, *12*, 607.
21. Mortazavi, M.A.; Knoesen; A.; Kowel, S.T.; Higgins, B.G.; Dienes, A. J. Opt. Soc. Am. **1989**, *B6*, 773.
22. Jeng, R.J.; Chen, Y.M.; Kumar, J.; Tripathy, S.K. Journ. Mac. Sci., Pure & Appl. Chem. **1992**, *A29*, 1115.
23. Mandal, B.K.; Chen, Y.M.; Lee, J.Y.; Kumar, J.; Tripathy, S.K. Appl. Phys. Lett. **1991**, *58*, 2459.
24. Lee, R.H.; Hsiue, G.H.; Jeng, R.J. J. Appl. Polym. Sci. **2001**, *79*, 1852.
25. Stevens, G.; Richardson, M. Polymer **1983**, *24*, 851.
26. Wung, C.J.; Lee, K.S.; Prasad, P.N.; Kim, J.C.; Jin, J.I.; Shim, H.K. Polymer **1992**, *33*, 4145.
27. Premachandra, J.; Kumudinie, C.; Zhao, W.; Mark, J.E. J. Sol-Gel Sci. Tech. **1996**, *7*, 163.
28. Wen, J.; Dhandapani, B.; Oyama, S.T.; Wilkes, G.L. Chem. Mater. **1997**, *9*, 1968.
29. Yang, Z.; Xu, C.; Wu, B.; Dalton, L.R.; Kalluri, S.; Steier, W.H.; Shi, Y.; Bechtel, J.H. Chem. Mater. **1994**, *6*, 1899.
30. Tsutsumi, N.; Moridhima, M.; Sakai, W. Macromolecules **1998**, *31*, 7764.
31. Hsiue, G.H.; Kuo, W.J.; Lin, C.H.; Jeng, R.J. Macromol. Chem. Phys. **2000**, 201, 2336.
32. Firestone, M.A.; Ratner, M.A.; Marks, T.J. Macromolecules **1995**, *28*, 6296.
33. Bristow, J.F.; Kalika, D.S. Macromolecules **1994**, *27*, 1808.
24. Kim, H.K.; Kang, S.J.; Choi, S.K.; Min, Y.H.; Yoon, C.S. Chem. Mater. **1999**, *11*, 779.
25. Kim, E.H.; Moon, I.K.; Kim, H.K.; Lee, M.H.; Han, S.G.; Yi, M.H.; Choi, K.Y. Polymer **1999**, *40*, 6157.

Received December 10, 2000
Revision received April 10, 2001